The potential meat flavoring derived from Maillard reaction products of rice protein isolate hydrolysate-xylose via the regulation of temperature and cysteine

Zuoyong Zhang [a,*], Jiayi Chen [a], Li Zheng [a], Jinlong Zhao [b], Na Guo [a], Xue Fang [a], Xuan Lu [a], Fangyan Zhang [a], Guilan Zhu [a,*]

[a] School of Biology and Food Engineering, Anhui Province Green Food Collaborative Technology Service Center for Rural Revitalization, Hefei Normal University, Hefei 230601, Anhui Province, PR China
[b] School of Food Engineering, Anhui Provincial Key Laboratory of Functional Agriculture and Functional Foods, Associated Discipline Key Laboratory of Whole Grain Nutrition and High-Value Utilization, Anhui Science and Technology University, Fengyang, 233100, Anhui Province, PR China

ARTICLE INFO

ABSTRACT

Maillard reaction products (MRPs) derived from rice protein isolate hydrolysate and D-xylose, with or without L-cysteine, were developed as a potential meat flavoring. The combined impact of temperature (80–140 °C) and cysteine on fundamental physicochemical characteristics, antioxidant activity, and flavor of MRPs were investigated through assessments of pH, color, UV–visible spectra, fluorescence spectra, free amino acids, volatile compounds, E-nose, E-tongue, and sensory evaluation. Results suggested that increasing temperature would reduce pH, deepen color, promote volatile compounds formation, and reduce the overall umami and bitterness. Cysteine addition contributed to the color inhibition, enhancement of DPPH radical-scavenging activity and reducing power, improvement in mouthfulness and continuity, reduction of bitterness, and the formation of sulfur compounds responsible for meaty flavor. Overall, MRPs prepared at 120 °C with cysteine addition could be utilized as a potential meat flavoring with the highest antioxidant activity and relatively high mouthfulness, continuity, umami, meaty aroma, and relatively low bitterness.

1. Introduction

Recently, plant-based meat analogues (PBMA) have gained popularity due to their nutritional, environmental, and sustainable characteristics, and it may be an effective strategy to solve the imbalance between the meat supply and human consumption (Sun et al., 2022). Thus, the development of stable, effective, and healthy meat flavorings using natural ingredients for PBMA has become a key issue. The Maillard reaction (MR) is a complex carbonyl-ammonia reaction between carbonyl groups of reducing sugars and amine groups of free amino acids, peptides, or proteins (Zhang et al., 2022). The resultant Maillard

reaction products (MRPs) not only significantly contribute to the color and meaty aroma of food (Sun et al., 2023), but also exhibit taste-enhancing properties, including mouthfulness, continuity, and umami (Chen et al., 2018). In addition, the MRPs, primarily melanoidins and some heterocyclic compounds, could exhibit excellent antioxidant properties in various foods by chelating metal ions and scavenging reactive oxygen species (Nooshkam, Varidi, & Bashash, 2019). Therefore, the MRPs might be used as a potential meat flavoring to enhance the flavor and antioxidant properties of various food systems, especially PBMA.

Nowadays, an increasing number of studies have focused on

exploring meat flavoring using various plant protein hydrolysates, including soybean protein (Yu et al., 2018), flaxseed protein (Wei, Thakur, Liu, Zhang, & Wei, 2018), camellia seed protein (Ni et al., 2021), pea protein (Zheng, Zhang, Zhang, Mujumdar, & Liu, 2023), wheat gluten protein (Sun et al., 2023) and so on. However, the utilization of rice protein hydrolysate in the creation of meat flavoring through the Maillard reaction is still restricted. Rice protein (RP) is an excellent plant-based protein with advantages of high nutritional and biological value, low allergen content, a large amount of essential amino acids, and easy digestibility (Cheng, Mu, Jiao, Xu, & Chen, 2021). It has been used as a functional ingredient in producing infant formula, cosmetics, and pharmaceutical adjuvants. Additionally, rice protein has a higher content of sulfur-containing amino acids (cysteine and methionine) than soybean, pea, and chickpea (Chiang, Yeo, Ong, & Henry, 2022). Cysteine can form specific Amadori rearrangement products with amino compounds in the initial phase of the Maillard reaction, which subsequently degrade into some sulfur-containing heterocyclic compounds responsible for the meaty aroma (Cao et al., 2017). Moderate addition of cysteine can confer potent inhibition of browning, enhance taste, and improve the DPPH radical scavenging ability and Fe^{3+} reducing power of MRPs (Xu, Zhang, Karangwa, & Xia, 2017; Zhao et al., 2019). Therefore, rice protein hydrolysate would be an ideal precursor for preparing Maillard reaction-based meat flavoring. The influence of cysteine on the sensory characteristics of MRPs would also be worth further study.

In addition, the reaction temperature was considered one of the most important parameters that could affect the antioxidant capacity and sensory characteristics of MRPs (Chen et al., 2018). Yu et al. (2018) reported that soybean peptides (1–3 kDa) heated at 120 °C for 2 h could exhibit a significant increase for DPPH radical scavenging activity, but peptides may undergo thermal degradation at higher temperatures, leading to a reduction in antioxidant activity. For another, Wei et al. (2019) found that higher temperatures (120 °C and 130 °C) could remarkably enhance the flavor formation in flaxseed protein hydrolysate MRPs, while a lower temperature (110 °C) was responsible for the generation of umami, mouthfulness, and continuity. Chen et al. (2018) reported that 125 °C was the optimal temperature for preparing mushroom hydrolysate MRPs with abundant volatile compounds and favorable sensory characteristics. Generally speaking, increasing temperature can enhance the production of flavor compounds, but it can also expedite reactions to an advanced stage, leading to the formation of unpleasant dark brown, burnt odors, and harmful substances such as acrylamide and hydroxymethylfurfural (Cheng et al., 2021). Thus, it is worthwhile to evaluate the effect of temperature on the changes in sensory attributes to adjust and enhance the meaty flavor of rice protein hydrolysate-based MRPs.

The objective of this study was to develop a potential meat flavoring derived from Maillard reaction products of rice protein isolate hydrolysate-xylose by regulating temperature and cysteine. The combined impact of temperature and cysteine addition on physicochemical properties (pH, color, UV–visible spectra, and fluorescence spectra), antioxidant activity (DPPH radical scavenging activity and reducing power), and flavor characteristics (free amino acids, volatile compounds, odor profile, taste profile, and overall sensory attributes) of MRPs were investigated. The correlations among free amino acids, volatile compounds, antioxidant activity, and sensory attributes were studied using principal component analysis (PCA) and partial least squares regression (PLSR) analysis to elucidate the key contributions of temperature and cysteine to the antioxidant activity and flavor of various products. The findings would provide a valuable reference for the development of potential rice protein isolate hydrolysate-based meat flavoring used to enhance the flavor of various foods.

2. Materials and methods

2.1. Materials and chemicals

Polished round-grained rice was purchased from local market (Hefei city, China). D-xylose and L-cysteine were both obtained from Shanghai Aladdin Biochemical Technology Co., Ltd. (Shanghai, China). The alkaline protease (200,000 U/g) and flavor protease (20,000 U/g) were purchased from Yuanye Biotechnology Co., Ltd. (Shanghai, China). 2,2-Diphenyl-1-picryl-hydrazyl (DPPH) was obtained from Sigma-Aldrich (St. Louis, MO, USA). All other analytical chemicals were provided by Sinopharm Chemical Reagent Co., Ltd. (Shanghai, China).

2.2. Preparation of rice protein isolate hydrolysate (RPIH)

Rice protein isolate (RPI) with a protein content of 86.85% (dry basis) was prepared using alkaline extraction (0.05 M NaOH) and acid precipitation (pH 4.6) according to a previous research (Cheng et al., 2021). The enzymatic hydrolysis of RPI was conducted in two steps following the method outlined by Yu et al. (2018) with some modifications. The RPI powder was dissolved in ultrapure water to achieve a final protein concentration of 8% (w/v). After incubating at 85 °C for 30 min, the RPI homogenate was hydrolyzed using alkaline protease (5000 U/g substrate protein) at 55 °C for 4.0 h at a pH of 10.0. Subsequently, the flavor protease (800 U/g substrate protein) was employed at 50 °C for 3.0 h at a pH of 6.5. After hydrolysis, the enzymes were inactivated by heating at 95 °C for 10 min. The supernatant was separated from the mixture by centrifuging at 6000 ×g for 20 min at 25 °C using a high-speed refrigerated centrifuge (TGL16M, Yancheng KaiT Experimental Instrument Co., Ltd., Jiangsu, China). The rice protein isolate hydrolysate (RPIH) was eventually obtained after vacuum freeze-drying for further use.

2.3. Preparation of RPIH Maillard reaction products (RPIH-MRPs)

The preparation of RPIH-MRPs was carried out using the method described by He et al. (2019) with some modifications. The 1.0 g of RPIH, 0.5 g of D-xylose, and 0.25 g of L-cysteine were dissolved in 10 mL of ultrapure water to obtain a Maillard reaction system. The initial pH of the reaction mixture was adjusted to 7.2 using 4 M NaOH. The mixture was then transferred into a 50 mL screw-sealed tube and heated at different temperatures of 80, 100, 120, and 140 °C in a thermostatic oil bath (DF-101Z, Shanghai LICHEN-BX Instrument Technology Co., Ltd., China) with magnetic stirring at 150 rpm. After a 2 h heating process, the samples were rapidly cooled using an ice slurry, and the corresponding MRPs (RHXC-MRPs) were named as RHXC-80, RHXC-100, RHXC-120, and RHXC-140, respectively. The controls (RHX-MRPs) were prepared using the same procedure but without cysteine addition, and labeled as RHX-80, RHX-100, RHX-120, and RHX-140, respectively. The obtained RPIH-Maillard reaction products were kept at −18 °C for the following analysis.

2.4. pH determination

The pH of RPIH-MRPs was measured by a pH meter (Model PHS-3C, Shanghai, China) at room temperature of 25 °C.

2.5. Color measurement

The color of RPIH-MRPs was measured using the Chroma Meter NR-200 (Shenzhen 3NH Technology Co., Ltd., Shenzhen, China). Before the measurement, the chroma meter was color-calibrated using black and white correction. The CIELAB parameters L* (brightness, with a higher value indicating higher lightness), a* (greenness (−) → redness (+)), and b* (blueness (−) → yellowness (+)) were measured. Ultrapure water was used as a control, and the total color difference (ΔE) was calculated

according to eq. (1) as shown below:

$$\Delta E = \sqrt{\Delta L^{*2} + \Delta a^{*2} + \Delta b^{*2}} \tag{1}$$

2.6. Spectral characteristics of RPIH-MRPs

The UV–visible spectra and fluorescence spectra were determined following our previous method (Zhang et al., 2022). The 3 mL of RPIH-MRPs with a 10-fold dilution were added to a quartz cuvette (12.5 × 12.5 × 45 mm) for spectral characteristics. UV–visible spectra of RPIH-MRPs were scanned from 200 nm to 800 nm using an UV-4802 spectrophotometer (Unico Shanghai Instrument Co., Ltd., Shanghai, China) with an interval of 1 nm. For fluorescence spectra, RPIH-MRPs were measured using a F97 PRO fluorescence spectrophotometer (Lengguang Technology, Shanghai, China) with an excitation wavelength of 347 nm and emission wavelengths ranging from 200 to 800 nm.

2.7. Determination of antioxidant properties

DPPH radical scavenging assay and reducing power assay were used to determine the antioxidant activity of RPIH-MRPs according to a previous method with some modifications (Zhang et al., 2022).

2.7.1. Determination of DPPH radical scavenging activity

The 1 mL of RPIH-MRPs solution was mixed with 2 mL of freshly prepared DPPH solution at a concentration of 0.1 mM in anhydrous ethanol. The reaction solution was vigorously mixed, followed by incubation at 25 °C for 30 min in the dark. The absorbance of the reaction solution was then measured at 517 nm using an UV-4802 spectrophotometer. DPPH radical scavenging activity was calculated using eq. (2):

$$\text{DPPH radical scavenging activity (\%)} = 1 - \frac{A_s - A_c}{A_b} \times 100\% \tag{2}$$

where A_s is the absorbance of the RPIH-MRPs sample, A_c is the absorbance of the control (anhydrous ethanol added instead of 0.1 mM DPPH solution), and A_b is the absorbance of the blank (distilled water added instead of the RPIH-MRPs sample).

2.7.2. Determination of reducing power

The 0.5 mL of RPIH-MRPs solution was mixed with 1.0 mL of sodium phosphate buffer (0.2 M, pH 6.6) and 1.0 mL of potassium ferricyanide (1%, w/v). The reaction mixture was incubated in a water bath at 50 °C for 20 min, followed by cooling down to room temperature and adding 1.0 mL of trichloroacetic acid (10%, w/v). The mixture was then centrifuged, and the obtained supernatant (1.0 mL) was treated with 1.0 mL of distilled water and 0.2 mL of ferric trichloride (0.1%, w/v). The absorbance of the reaction solution was measured at 700 nm. The reducing power of the blank (distilled water instead of 1% potassium ferricyanide) was taken as the reference value. The higher absorbance of the reaction mixture indicated greater reducing power.

2.8. Free amino acids (FAA) determination

The determination of FAA in RPIH-MRPs was conducted using an automatic amino acid analyzer (L-8800 , Hitachi Co., Tokyo, Japan) according to the method of Yu et al. (2018). To avoid testing interference from proteins and/or peptides, an equal volume of cold trichloroacetic acid (10%, w/v) was added to the samples, followed by an overnight incubation at 4 °C. After refrigerated centrifugation at 6000 ×g for 15 min at 4 °C, the obtained supernatant was filtered through a 0.22 μm nylon syringe filter for FAA determination. Moreover, a calibration curve was obtained using the standard mixture of amino acids from Sigma-Aldrich (St. Louis, MO), and the content of each amino acid was calculated based on its retention time and peak area.

2.9. Volatile compounds determination by SPME/GC–MS

The volatile compounds of RPIH-MRPs were analyzed using GC–MS (7890 A-5975C model, Agilent Technology Inc., Palo Alto, CA, USA) equipped with a DB-WAX capillary column (30 m × 0.25 mm × 0.25 μm, J&W Scientific, Folsom, CA, USA). A solid phase micro-extraction (SPME) fiber (50/30 μm DVB/CARBOXEN-PDMS, Supelco Co., USA) was used for the volatile compounds extraction. A 20 mL glass vial containing 5 mL of RPIH-MRPs was sealed with a PTFE/BYTL septum and equilibrated at 50 °C for 5 min. Subsequently, it was exposed to a SPME fiber for 25 min to facilitate the adsorption of volatiles in the headspace. After extraction, the SPME fiber was desorbed into the GC injection port at 250 °C for 7 min. The column temperature program was 40 °C (for 3 min), 40–80 °C (5 °C/min), 80–160 °C (10 °C/min), 160–175 °C (2 °C/min), 175–230 °C (10 °C/min), and 230 °C held for 7 min according to a previous report (Zhang et al., 2022). Helium as the carrier gas was set at a flow rate of 1.8 mL/min and conducted in a splitless mode. The MS conditions were as follows: electron impact ionization mode, electron energy 70 ev, ion source temperature 230 °C, interface temperature 250 °C, quadrupole temperature 150 °C, and scan range of 29–400 m/z. The peak was identified based on the National Institute of Standards and Technology (NIST) 08 MS library, and relative content of the special compound was computed via the peak area.

2.10. Instrumental sensory evaluation

Instrumental sensory evaluation, including E-nose and E-tongue, was performed according to the method of Yu et al. (2018) with some modifications.

2.10.1. E-nose analysis

The odor characteristics of RPIH-MRPs were analyzed by a PEN3 model Portable Electronic Nose (Airsense Analytics GmbH, Schwerin, Germany) equipped with 10 metal oxide sensors. The 2 mL of samples were added to a 50 mL glass vial sealed with a PTFE/BYTL septum and incubated at 50 °C for 15 min. After incubation, the headspace gas was extracted using a gas injection needle and analyzed by E-nose. The clean air was used as the blank sample in the experiment, and all samples were repeated in triplicate.

2.10.2. E-tongue analysis

The taste characteristics of RPIH-MRPs were analyzed using a TS-5000Z Electronic Tongue (Intelligent Sensor Technology Co., Ltd., Japan). The 5 mL of RPIH-MRPs solution were mixed with 45 mL of an umami solution consisting of 0.5% (w/v) sodium chloride (NaCl) and 1.0% (w/v) monosodium glutamate (MSG). The reference solution was a umami solution (50 mL) without RPIH-MRPs addition. Each sample was measured in triplicate.

2.11. Descriptive sensory evaluation

The descriptive sensory evaluation was carried out according to the procedure of Wei et al. (2018) with some modifications. For sensory evaluation, 12 trained panelists (6 males and 6 females, aged within 18–40 years) were selected from School of Biology and Food Engineering, Hefei Normal University (Hefei, China) by confirming the criteria for descriptive analysis. The sensory evaluation was conducted after receiving approval from the Hefei Normal University Ethics Committee. It can be confirmed that the appropriate protocols for protecting the rights and privacy of all participants were utilized during the execution of the research, e.g., no coercion to participate, full disclosure of study requirements and risks, written or verbal consent of participants, no release of participant data without their knowledge, and the ability to withdraw from the study at any time. The nine descriptors (mouthfulness, continuity, umami, bitterness, salty, meaty, caramel, burnt, and overall acceptance) were chosen to evaluate the flavor profiles of RPIH-

MRPs. The intensity of the descriptive terms was rated on a 9-point scale, anchored from "none" at 1 point to "extreme" at 9 point. The reference materials were prepared as follows: 10.0 g of bouillon cube for mouthfulness and continuity attributes, 4.0 mM of MSG for umami taste, 1.5 mM of caffeine for bitter taste, 2.0 mM of NaCl for salty taste, 20 g of lean chicken roasted at 120 °C or 250 °C for 30 min for meaty flavor or burnt attribute, and 2.5 g of burning white sugar in 50 mL water for caramel-like odor. The RPIH-MRPs (1.0%, v/v) were individually dissolved in an umami solution consisting of 1.0% (w/v) MSG and 0.5% (w/v) NaCl as the test solutions. All test solutions were adjusted to pH 7.0, and then completely sealed and incubated at 60 °C in a water bath. Then, sensory evaluation was conducted in a sensory laboratory following the guidelines and conditions outlined in ISO 8589:2007.

2.12. Statistical analysis

The data were expressed as mean value ± standard deviation (SD) with at least three repeats unless specified otherwise. Single-factor ANOVA was performed using SPSS version 22.0 (Chicago, IL, USA)

under Tukey's multiple comparison, and statistical significance was considered at $p < 0.05$. The heat map of volatile compounds was displayed using Origin 2018 software (OriginLab Corporation, Northampton, MA, USA). The flavor wheel of volatile compounds was performed using Microsoft Office Excel 2013 (Microsoft Corporation, Redmond, Washington, USA). PCA and PLSR analysis were performed using the Unscrambler X version 10.4 (CAMO ASA, Oslo, Norway).

3. Results and discussion

3.1. Changes in pH

As shown in Fig. 1a, the terminal pH in RHXC-MRPs significantly ($p < 0.05$) decreased from 6.64 to 5.24 with a rise in temperature from 80 °C to 140 °C, while that in RHX-MRPs significantly ($p < 0.05$) reduced from 5.87 to 4.47, suggesting that increasing temperature would accelerate the MR rate. Additionally, RHXC-MRPs always had a lower pH value compared to the corresponding RHX-MRPs, which might be attributed to the degradation of cysteine, leading to the generation of
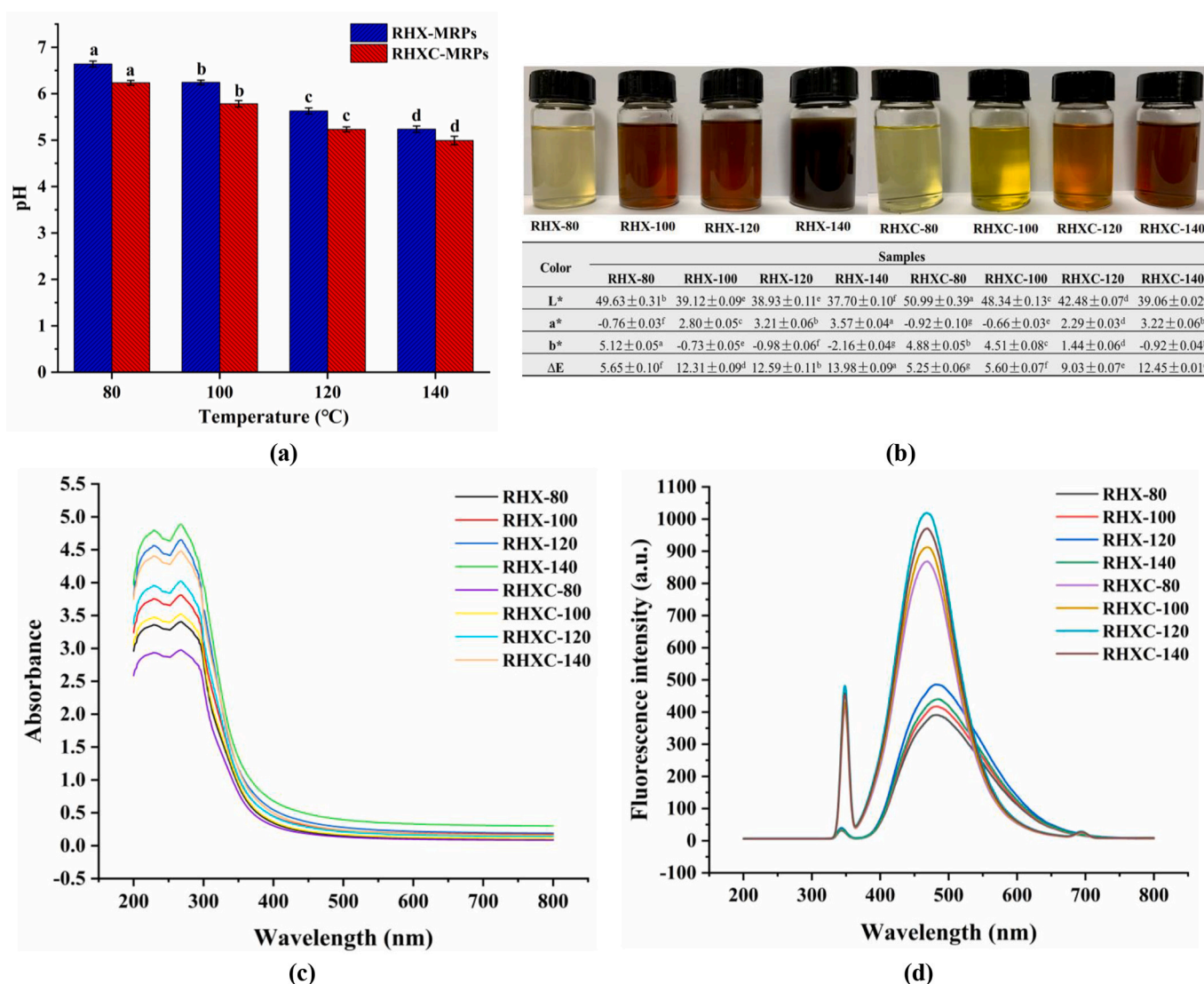

Color	Samples							
	RHX-80	RHX-100	RHX-120	RHX-140	RHXC-80	RHXC-100	RHXC-120	RHXC-140
L*	49.63±0.31^b	39.12±0.09^e	38.93±0.11^e	37.70±0.10^f	50.99±0.39^a	48.34±0.13^c	42.48±0.07^d	39.06±0.02^e
a*	-0.76±0.03^f	2.80±0.05^c	3.21±0.06^b	3.57±0.04^a	-0.92±0.10^g	-0.66±0.03^e	2.29±0.03^d	3.22±0.06^b
b*	5.12±0.05^a	-0.73±0.05^e	-0.98±0.06^f	-2.16±0.04^g	4.88±0.05^b	4.51±0.08^c	1.44±0.06^d	-0.92±0.04^f
ΔE	5.65±0.10^f	12.31±0.09^d	12.59±0.11^b	13.98±0.09^a	5.25±0.06^g	5.60±0.07^f	9.03±0.07^e	12.45±0.01^c

(a) **(b)**

(c) **(d)**

Fig. 1. Effects of temperature and cysteine on the fundamental physicochemical properties of Maillard reaction products derived from rice protein isolate hydrolysate and xylose: (a) pH, (b) color, (c) ultraviolet absorption spectra, and (d) fluorescence spectra. Values followed by different lowercase letters mean statistically significant ($p < 0.05$) differences among different products. RHX-MRPs mean rice protein isolate hydrolysate-xylose Maillard reaction products, and RHX-80, RHX-100, RHX-120, and RHX-140 represent RHX-MRPs prepared at different temperatures of 80, 100, 120, and 140 °C, respectively. RHXC-MRPs mean rice protein isolate hydrolysate-xylose-cysteine Maillard reaction products, and RHXC-80, RHXC-100, RHXC-120, and RHXC-140 represent RHXC-MRPs prepared at different temperatures of 80, 100, 120, and 140 °C, respectively.

more acidic compounds (Shen et al., 2021). The pH changes were consistent with a previous report indicating that increasing temperature could enhance the degradation of sugars, free amino acids, and peptides to generate formic and acetic acids, and the consumption of amino groups could also increase the exposure rate of free carboxyl groups in the MR system (Sun et al., 2023).

3.2. Changes in color

With the increase in heating temperature, the L* value decreased significantly ($p < 0.05$), while the a* and b* values exhibited a significant ($p < 0.05$) increasing trend (Fig. 1b), suggesting that the color of RPIH-MRPs shifted gradually from light yellow to dark brown. The browning color of the RPIH-MRPs might be attributed to the caramelization and melanoidin formation under high temperatures (Xiao, Woo, Hu, Xiong, & Zhao, 2021). Furthermore, the ΔE values of both RHX-MRPs and RHXC-MRPs decreased significantly ($p < 0.05$) with the increase in temperature. The RHX-MRPs exhibited notably higher ΔE values than the corresponding RHXC-MRPs, indicating that adding cysteine could restrain brownish polymers formation. The brown-inhibiting effect of cysteine could be ascribed to its free thiol group with special redox and nucleophilic characteristics that can readily react with carbonyl intermediates, thereby suppressing pigmentation (Zhu et al., 2023).

3.3. Spectral analysis of RPIH-MRPs

UV–vis spectroscopy can be used to monitor and characterize the progress of Maillard reaction. As presented in Fig. 1c, there were two absorption peaks in all RPIH-MRPs at 200–300 nm, indicating the formation of Schiff base (Zhang et al., 2022). The maximum absorption peaks of RPIH-MRPs were observed at 228 nm and 267 nm. As reported, MRPs prepared from four sugars (glucose/fructose/xylose/ribose) with tyrosine, histidine, phenylalanine, glutamic acid, glutamine, aspartic acid, and asparagine showed two absorption peaks at around 265 nm and 215 nm, and MRPs derived from pentose (ribose and xylose) and amino acids exhibited a sharp absorption peak at around 265 nm (Yu, Zhao, Hu, Zeng, & Bai, 2012). Moreover, the absorbance of the UV–vis curve increased gradually with a rise in temperature, and the values were consistently in the order of RHXC-140 > RHXC-120 > RHXC-100 > RHXC-80 and RHX-140 > RHX-120 > RHX-100 > RHX-80, suggesting that high temperatures would accelerate the MR and intensify browning. The absorbance of RHXC-MRPs was lower than that of the corresponding RHX-MRPs because cysteine degradation could lower the pH, ultimately inhibiting the browning rate and reducing the MR degree (Jin et al., 2018).

As clarified in fluorescence spectroscopy (Fig. 1d), each sample exhibited a higher fluorescence intensity in the range of 400–600 nm after excitation at a wavelength of 347 nm, indicating the formation of fluorescent compounds. These compounds may be a Schiff base conjugated with an electron-donating group, a nitrogen-containing compound, or a cyclic unsaturated carbonyl compound (Huang, Cui, Hayat, Zhang, & Ho, 2022). The fluorescence intensities of RPIH-MRPs increased with the elevated temperatures from 80 °C to 120 °C, suggesting the gradual accumulation of fluorescent compounds (Zhang et al., 2022). The fluorescent compounds formed in the early stage can act as precursors for browning compounds and may be converted to melanoidins as the MR proceeds (Fu et al., 2020). When the temperature reached 140 °C, the fluorescence intensity began to decrease due to the conversion of fluorescent compounds to melanoidins. Moreover, RHXC-MRPs showed a greater fluorescence intensity in contrast to RHX-MRPs, which might be ascribed to the brown-inhibiting effect of cysteine, resulting in the accumulation of fluorescent compounds.

3.4. Antioxidant activity analysis

As shown in Fig. 2a and b, the DPPH radical scavenging ability and Fe^{3+} reducing power of RPIH-MRPs initially increased and then decreased with increasing temperature. The strongest antioxidant ability was observed at 120 °C with a DPPH radical scavenging ability of 44.43% and a reducing power of 0.551 in RHX-120, whereas in RHXC-120, these values were 53.87% and 0.603, respectively. RHXC-MRPs showed higher antioxidant ability compared to RHX-MRPs, which was consistent with a previous research indicating that MRPs prepared with cysteine had the stronger antioxidant activity (Xu et al., 2017). The antioxidant mechanism may be related to the formation of melanoidins, antioxidant peptides, the MR intermediate products, reductive ketones, N- and S-containing heterocyclic compounds, and some other substances that can provide hydrogen atoms (Ni et al., 2021). Heterocyclic volatile
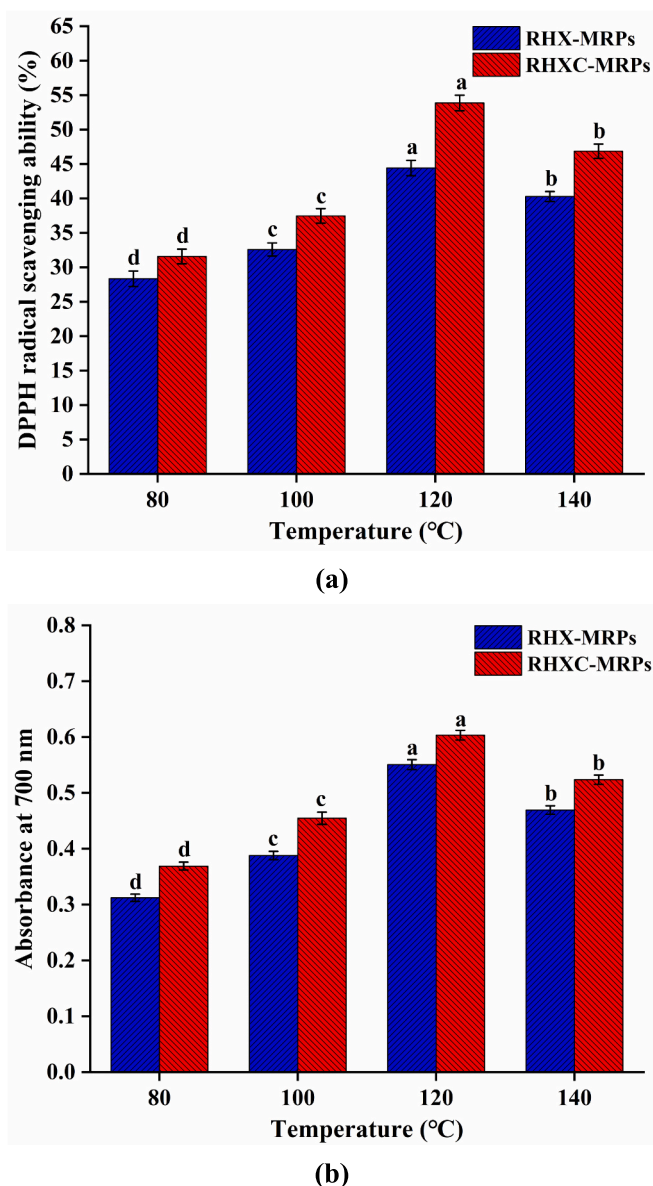
(a)

(b)

Fig. 2. Effects of temperature and cysteine on the antioxidant activity of Maillard reaction products derived from rice protein isolate hydrolysate and xylose: (a) DPPH radical scavenging activity and (b) reducing power at 700 nm. Values followed by different lowercase letters mean statistically significant ($p < 0.05$) differences among different products. RHX-MRPs mean rice protein isolate hydrolysate-xylose Maillard reaction products, and RHXC-MRPs mean rice protein isolate hydrolysate-xylose-cysteine Maillard reaction products.

compounds, such as pyrroles, furans, thiophenes, thiazoles, and pyrazines, have been reported to possess certain antioxidant activities (Yu et al., 2013). Compounds containing a thiol group may also demonstrate increased antioxidant activity by scavenging free radicals (e.g., peroxyl) or decomposing hydroperoxides (Shakoor, Zhang, Xie, & Yang, 2022).

3.5. Free amino acids (FAA) analysis

The FAA had a positive contribution to the taste attribute of the MRPs and can be divided into three categories, including umami (Asp and Glu), bitterness (Met, Ile, Leu, Tyr, Phe, Val, His, and Arg), and sweetness (Lys, Pro, Ala, Ser, Thr, and Gly) (Cao et al., 2023). As illustrated in Table 1, when the temperature increased from 80 °C to 100 °C, the contents of umami, bitter, and sweet amino acids gradually increased, probably due to the dominance of thermal degradation of rice protein peptides. However, as the temperature increased from 100 °C to 140 °C, the FAA content began to decrease, which might be attributed to the FAA thermal degradation, peptide crosslinking, and/or grafting with reducing sugars to form volatiles or Amadori compounds (Xiao et al., 2021). Moreover, RHXC-MRPs seemed to retain more umami FAA and bitter FAA than those in RHX-MRPs, which can be explained by the fact that cysteine could suppress FAA-sugar and/or FAA-peptide crosslinking reactions to prevent the formation of non-volatile compounds (He et al., 2019). Overall, the reaction conditions involving a heating temperature of 100 °C with cysteine addition (RHXC-100) would be advantageous for producing the highest levels of umami, bitter, and sweet amino acids, followed by the conditions of 120 °C with cysteine addition (RHXC-120).

3.6. Volatile compounds analysis

To explore the flavor characteristics of RHX-MRPs and RHXC-MRPs, two three-tiered flavor wheels were constructed based on a total of 132 volatile compounds belonging to different structure and flavor categories (Fig. 3), mainly including 55 aliphatic oxygen-containing compounds (14 aldehydes, 12 ketones, 11 alcohols, 12 acids, and 6 esters), 13 furans, 23 nitrogenous heterocyclic compounds (9 pyrazines, 8 pyrroles, and 6 pyridines), and 41 sulfur-containing compounds (19 thiophenes, 8 thiazoles, 7 thiols, and 7 sulfides) (Fig. 4a). The high temperature in the range of 120–140 °C was beneficial for the formation of volatile compounds, as indicated by the area occupied on the flavor wheel. There were more aldehydes, ketones, alcohols, pyrazines, and furans in RHX-120 and RHX-140 (Fig. 3a), while more thiophenes, thiazoles, thiols, and sulfides were newly formed in RHXC-120 and RHXC-140 (Fig. 3b), indicating that high temperature without cysteine addition would promote the generation of aliphatic oxygen-containing compounds, sulfur-deprived furans, and nitrogenous heterocyclic compounds, and adding cysteine was favorable to the production of sulfur-containing compounds.

As shown in Fig. 4b, oxygen-containing compounds were primarily derived from the oxidation of fatty acids or lipids, which had a high odor threshold and usually had no direct contribution to the meaty flavor (Shen et al., 2021). Furans and furan derivatives, mainly generated from carbohydrate degradation or caramelization, Amadori rearrangement, and fatty acid oxidation, were usually exhibited sweet, fruity, nutty, and caramel-like odor notes (Zhang, Ji, Peng, Ji, & Gao, 2020). As displayed in Fig. 4c, furfural, mainly derived from xylose, was the most abundant furan detected in RHX-120 and RHX-140, which was reported to have a baked potato flavor and a sweet taste (Zheng, Wei, et al., 2023). The increase in furfural content may be due to the competitive synthesis of fatty aldehydes and xylose with cysteine, eventually leading to the aggravation of xylose degradation during the thermal reaction (Zhang et al., 2021). 2-Pentylfuran was a product of the oxidation of n-6 PUFAs, while 2-propylfuran was derived from linolenate oxidation, and these compounds were detected more in RHX-MRPs and could impart meat lipid oxidation, chocolate, and caramel aromas (Zhang et al., 2020).

The relative contents of nitrogen-containing heterocyclic compounds, mainly pyrazines, pyridines, and pyrroles, were presented in Fig. 4d. Pyrazines, derived from the interaction between α-dicarbonyls

Table 1
Effects of temperature and cysteine on the free amino acids of RHX-MRPs and RHXC-MRPs.

Amino acids	The free amino acids concentration (mg/100 mL)							
	RHX-80	RHX-100	RHX-120	RHX-140	RHXC-80	RHXC-100	RHXC-120	RHXC-140
Asp	19.83 ± 0.16^f	24.13 ± 0.11^b	21.72 ± 0.18^d	14.79 ± 0.18^h	21.07 ± 0.16^e	28.93 ± 0.11^a	23.26 ± 0.11^c	18.04 ± 0.18^g
Glu	22.58 ± 0.22^e	27.82 ± 0.16^c	24.11 ± 0.17^d	17.78 ± 0.14^g	24.47 ± 0.15^d	32.55 ± 0.14^a	30.65 ± 0.13^b	21.19 ± 0.18^f
Total umami amino acids	42.41 ± 0.38^e	51.95 ± 0.27^c	45.83 ± 0.34^d	32.57 ± 0.32^g	45.54 ± 0.30^d	61.48 ± 0.25^a	53.91 ± 0.21^b	39.23 ± 0.35^f
Met	1.30 ± 0.08^{cd}	1.66 ± 0.09^b	1.37 ± 0.06^c	1.15 ± 0.08^d	1.64 ± 0.08^b	2.01 ± 0.06^a	1.55 ± 0.08^b	1.23 ± 0.06^{cd}
Ile	ND	ND	ND	1.26 ± 0.08^b	ND	ND	ND	1.95 ± 0.09^a
Leu	7.67 ± 0.19^d	10.29 ± 0.17^b	8.83 ± 0.13^c	6.75 ± 0.19^e	8.86 ± 0.12^c	12.27 ± 0.16^a	10.18 ± 0.16^b	9.07 ± 0.13^c
Tyr	6.61 ± 0.23^e	8.37 ± 0.12^b	7.50 ± 0.17^d	5.71 ± 0.15^g	7.87 ± 0.13^c	9.83 ± 0.12^a	8.63 ± 0.17^b	6.18 ± 0.11^f
Phe	31.01 ± 0.27^e	35.27 ± 0.22^b	32.69 ± 0.21^c	27.06 ± 0.15^g	32.09 ± 0.17^d	38.99 ± 0.25^a	35.39 ± 0.11^b	29.29 ± 0.21^f
Val	6.31 ± 0.21^g	6.55 ± 0.12^{fg}	7.84 ± 0.12^e	6.75 ± 0.11^f	8.64 ± 0.11^c	9.04 ± 0.12^b	9.85 ± 0.11^a	8.18 ± 0.12^d
His	2.12 ± 0.06^c	2.62 ± 0.09^b	2.18 ± 0.09^c	1.14 ± 0.08^d	3.10 ± 0.04^a	3.13 ± 0.07^a	3.17 ± 0.07^a	2.14 ± 0.09^c
Arg	1.25 ± 0.13^d	1.21 ± 0.08^d	1.08 ± 0.05^{de}	0.93 ± 0.05^e	2.25 ± 0.08^b	2.74 ± 0.07^a	2.28 ± 0.08^b	1.53 ± 0.07^c
Total bitter amino acids	56.26 ± 0.41^g	65.98 ± 0.11^c	61.48 ± 0.29^e	50.74 ± 0.27^h	64.44 ± 0.33^d	78.0 ± 0.24^a	71.05 ± 0.32^b	59.57 ± 0.61^f
Lys	14.35 ± 0.12^b	12.21 ± 0.11^d	9.35 ± 0.16^f	7.32 ± 0.12^h	15.20 ± 0.14^a	12.93 ± 0.12^c	10.19 ± 0.12^e	8.47 ± 0.10^g
Pro	ND	ND	ND	0.33 ± 0.07^b	ND	ND	ND	0.48 ± 0.05^a
Ala	9.64 ± 0.15^e	11.58 ± 0.14^c	10.56 ± 0.13^d	8.12 ± 0.09^g	10.78 ± 0.14^d	13.95 ± 0.18^a	12.51 ± 0.16^b	8.86 ± 0.12^f
Ser	5.28 ± 0.14^e	6.33 ± 0.14^c	5.23 ± 0.12^e	4.17 ± 0.11^f	5.97 ± 0.11^d	8.45 ± 0.12^a	7.65 ± 0.14^b	6.18 ± 0.14^{cd}
Thr	ND	ND	0.71 ± 0.08^c	0.54 ± 0.06^d	ND	ND	1.28 ± 0.08^a	0.86 ± 0.08^b
Gly	1.58 ± 0.09^e	2.19 ± 0.15^c	2.54 ± 0.08^b	0.65 ± 0.07^g	1.86 ± 0.08^d	2.55 ± 0.08^b	2.87 ± 0.09^a	1.07 ± 0.06^f
Total sweet amino acids	30.85 ± 0.26^e	32.31 ± 0.26^d	28.39 ± 0.24^f	21.12 ± 0.15^h	33.80 ± 0.12^c	37.88 ± 0.46^a	34.49 ± 0.42^b	25.91 ± 0.22^g
Cys	ND	ND	ND	ND	60.12 ± 0.09^a	52.09 ± 0.25^b	32.24 ± 0.13^c	23.47 ± 0.15^d
Total amino acids	129.52 ± 0.35^g	150.24 ± 0.53^d	135.70 ± 0.87^f	104.43 ± 0.21^h	203.90 ± 0.78^b	229.46 ± 0.99^a	191.70 ± 1.07^c	148.17 ± 0.37^e

Results are expressed as mean ± standard deviation ($n = 3$), values followed by different superscript lowercase letters in the same column mean statistically significant ($p < 0.05$) differences. RHX-MRPs mean rice protein isolate hydrolysate-xylose Maillard reaction products, and RHX-80, RHX-100, RHX-120, and RHX-140 represent RHX-MRPs prepared at different temperatures of 80, 100, 120, and 140 °C, respectively. RHXC-MRPs mean rice protein isolate hydrolysate-xylose-cysteine Maillard reaction products, and RHXC-80, RHXC-100, RHXC-120, and RHXC-140 represent RHXC-MRPs prepared at different temperatures of 80, 100, 120, and 140 °C, respectively.
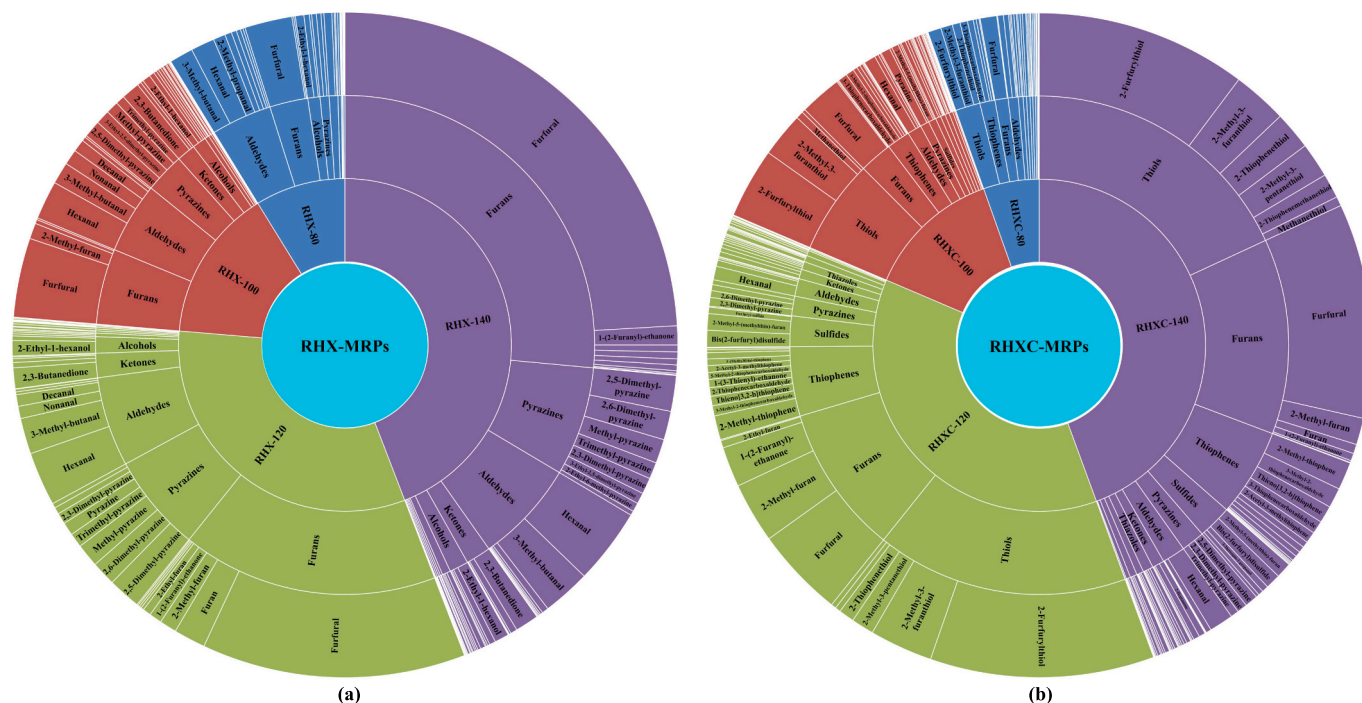
(a)

(b)

Fig. 3. Flavor wheel of RHX-MRPs and RHXC-MRPs based on volatile compounds. RHX-MRPs mean rice protein isolate hydrolysate-xylose Maillard reaction products, and RHX-80, RHX-100, RHX-120, and RHX-140 represent RHX-MRPs prepared at different temperatures of 80, 100, 120, and 140 °C, respectively. RHXC-MRPs mean rice protein isolate hydrolysate-xylose-cysteine Maillard reaction products, and RHXC-80, RHXC-100, RHXC-120, and RHXC-140 represent RHXC-MRPs prepared at different temperatures of 80, 100, 120, and 140 °C, respectively.

and amines via Strecker degradation during the Maillard reaction, were the most important aroma compounds contributing to the nutty, cocoa, coffee, and roast meat-like odors (Yu, Seow, Ong, & Zhou, 2017). A significant amount of pyrazine compounds were produced in RHX-120 and RHX-140, whereas only 2,3-dimethyl-pyrazine, 2,5-dimethyl-pyrazine, 2,6-dimethyl-pyrazine, and trimethyl-pyrazine were identified in RHXC-120 and RHXC-140. Moreover, pyridine and substituted pyridines may be produced from the condensation reaction of aldehydes, ketones, or α,β-unsaturated carbonyl compounds with ammonia, potentially contributing to the roasted burnt odor (He et al., 2019; Zhang et al., 2022). More pyridines were produced in RHX-120, RHX-140, and RHXC-140. Some pyrroles have a caramel and sweet odor, which can be formed by the aldol condensation of acetaldehyde with α-amino-carbonyl produced during Strecker degradation (Lee, Kwon, Kim, & Kim, 2011). The MR system without cysteine at high temperatures appeared to promote the formation of pyrrole compounds.

As presented in Fig. 4e, a large amount of sulfur-containing compounds were predominantly identified in RHXC-MRPs, and their relative content substantially increased with an increase in temperature. Thiophene compounds may be formed by the reaction between carbonyl compounds or unsaturated aliphatic aldehydes with hydrogen sulfide, followed by cyclization and rearrangement (Yu, Tan and Wang, 2012). The 2-methyl-thiophene, 2,5-dimethyl-thiophene, 3-(methylthio)-thiophene, 2-thiophenecarboxaldehyde, 3-methyl-2-thiophenecarbox-aldehyde, 5-methyl-2-thiophenecarboxaldehyde, 2-acetyl-3-methylthiophene, 1-(3-thienyl)-ethanone, and thieno[3,2-*b*]thiophene had a characteristic meaty flavor (Du et al., 2023; Xu et al., 2011), and these compounds were found in RHXC-120 and RHXC-140 with a dominant content. Thiazoles frequently contributed to the meaty flavor, cracker-like, and popcorn-like aromas in processed foods (Wang et al., 2021). The formation of alkyl thiazoles may involve the reaction of α-dicarbonyls or hydroxyketones with H_2S and NH_3, and an aldehyde (Zhang et al., 2022). There were plenty of thiazole, 2-methyl-thiazole, 5-methyl-thiazole, aminothiazole, and 2-acetylthiazole identified in RHXC-120 and RHXC-140. Thiol compounds were formed by H_2S

produced during the degradation of sulfur-containing amino acids in the Maillard reaction (Wei et al., 2019). Among them, 2-methyl-3-furanthiol was responsible for roasted, coffee-like, and meaty aromas, and 2-furfur-ylthiol was the key odorant in cooked meat (Zheng et al., 2023). Furthermore, sulfur-substituted furans such as furfuryl sulfide, bis(2-furfuryl)disulfide, and 2-methyl-5-(methylthio)-furan have been found to make a significant contribution to a strong meaty flavor or roasted note (Zhang et al., 2022). They were detected in all RHXC-MRPs, and RHXC-120 had the highest content.

In brief, Cys was an indispensable precursor for the generation of meaty flavor. The rice protein isolate hydrolysate-xylose MR system heated at high temperature with cysteine addition would promote the formation of more sulfur-containing compounds, including sulfur-containing furans, thiophenes, thiazoles, thiols, and sulfides.

3.7. Analysis of odor attributes using E-nose

There were 10 sensor probes in an E-nose system consisted of W1C (sensitive to aromatic compounds, benzene), W5S (highly sensitive to nitrogen oxides), W3C (sensitive to aromatic compounds, ammonia), W6S (sensitive to hydrogen), W5C (sensitive to olefin, short-chain aromatic compounds), W1S (sensitive to methyl), W1W (sensitive to sulfur compounds), W2S (sensitive to alcohols, aldehydes, and ketones), W2W (sensitive to organic sulfides), and W3S (sensitive to long-chain alkanes). As depicted in the radar diagram of E-nose (Fig. 5a), RPIH-MRPs exhibited minor response values in W1C, W3C, W6S, W5C, and W3S, whereas it displayed a strong response to W5S, W1S, W1W, W2S, and W2W, indicating the formation of higher contents of alcohols, aldehydes, ketones, nitrogen oxides, and sulfur-containing compounds. The signal strength of W5S, W1S, W1W, W2S, and W2W significantly ($p <$ 0.05) increased as the temperature rose from 80 to 140 °C. RHXC-MRPs showed higher response values for W1W and W2W, suggesting that adding cysteine favored the formation of sulfur-containing compounds such as thiophenes, thiazoles, thiols, and sulfides. The findings were consistent with the results of previous GC–MS analysis.
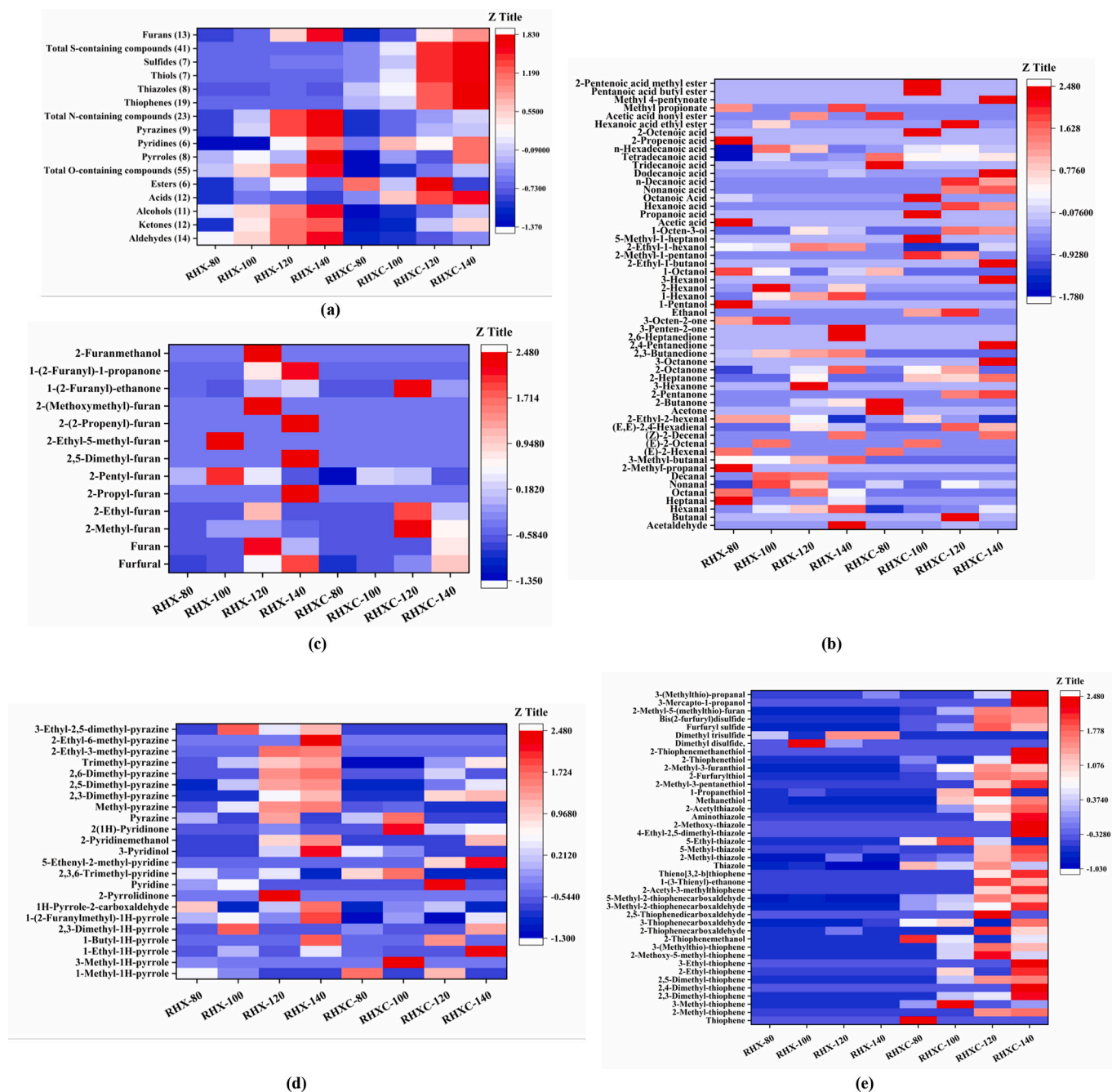
Fig. 4. Heat map of volatile compounds formed in RHX-MRPs and RHXC-MRPs: (a) overview of all kinds of volatile compounds, (b) aliphatic oxygen-containing compounds, (c) non sulfur-containing furan compounds, (d) nitrogenous heterocyclic compounds, and (e) sulfur-containing compounds. The change in color from blue to red in the heat map represents a gradual increase in the relative content of volatile compounds. RHX-MRPs mean rice protein isolate hydrolysate-xylose Maillard reaction products, and RHX-80, RHX-100, RHX-120, and RHX-140 represent RHX-MRPs prepared at different temperatures of 80, 100, 120, and 140 °C, respectively. RHXC-MRPs mean rice protein isolate hydrolysate-xylose-cysteine Maillard reaction products, and RHXC-80, RHXC-100, RHXC-120, and RHXC-140 represent RHXC-MRPs prepared at different temperatures of 80, 100, 120, and 140 °C, respectively. (For interpretation of the references to color in this figure legend, the reader is referred to the web version of this article.)

PCA is a multivariate statistical tool used to explain the differences between samples by extracting maximum information from the main influencing variables of the sample spatial distribution (Zhang et al., 2022). As shown in the score plot (Fig. 5c), PC1 and PC2 had eigenvalues of 75% and 20%, respectively. These two principal components explained 95% of the overall variance, indicating that they could reflect the most information of the samples. The blank groups were distributed to the right of the score plot, RHX-MRPs groups were distributed in the upper left, and RHXC-MRPs groups were distributed in the lower left,

indicating that the blank, RHX-MRPs, and RHXC-MRPs were well differentiated from each other. Meanwhile, RPIH-MRPs prepared at the same temperature were clustered together, and there was an obvious distribution difference between different groups as the temperature changed. Therefore, temperature and cysteine had significant effects on the odor attributes of RPIH-MRPs, which can be effectively discriminated by an E-nose system. As depicted in the loading plot (Fig. 5d), PC1 and PC2 accounted for 62% of the total variance. The blank groups exhibited a strong correlation with the sensor signals of W1C, W3C,
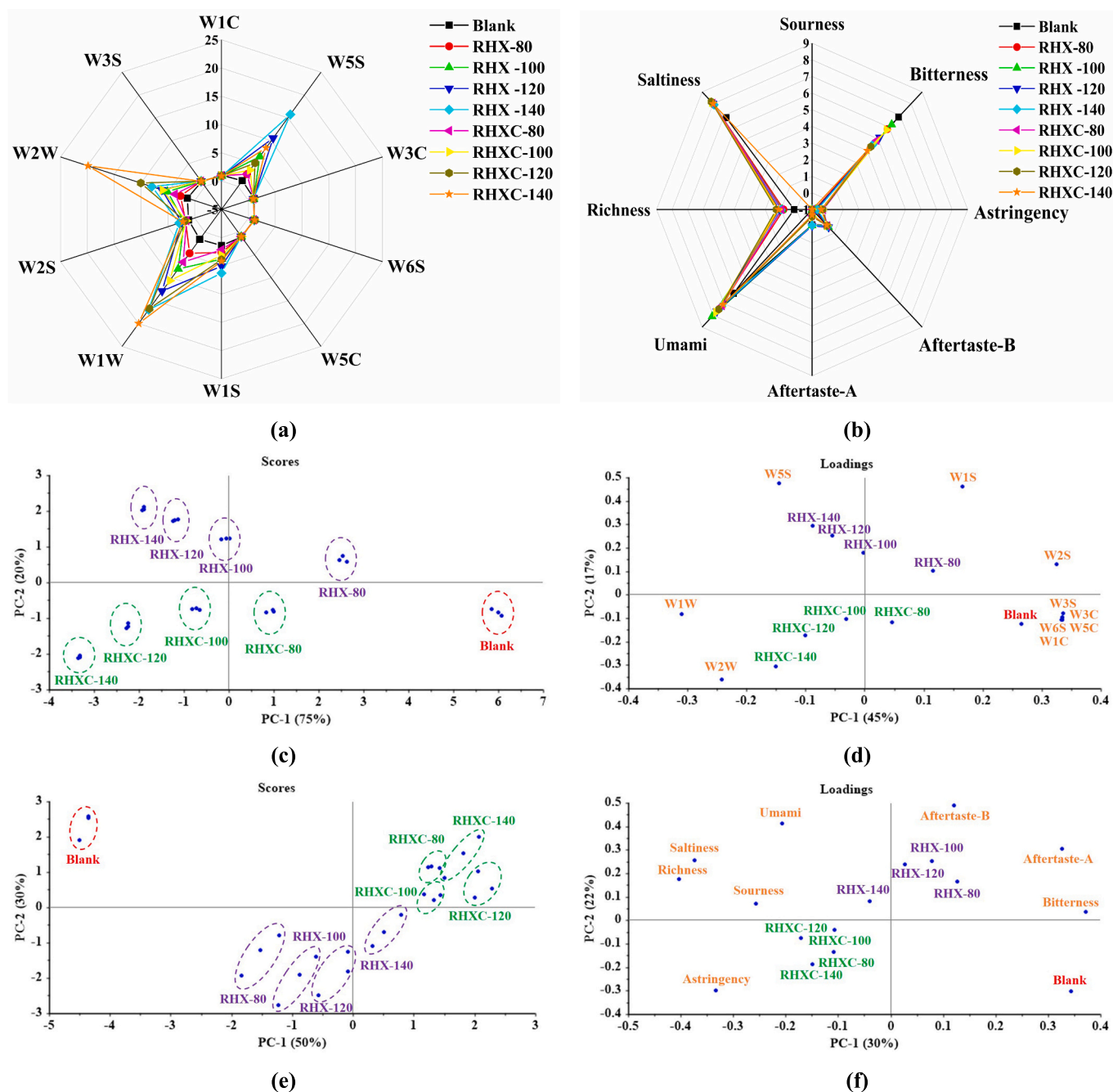
(a)

(b)

(c)

(d)

(e)

(f)

Fig. 5. The odor and taste attributes of RHX-MRPs and RHXC-MRPs analyzed using instrumental sensory analysis system: (a) radar diagram, (c) score plot and (d) loading plot of PCA for E-nose; (b) radar diagram, (e) score plot and (f) loading plot of PCA for E-tongue. There are 10 sensor probes in an E-nose system consisted of W1C (sensitive to aromatic compounds, benzene), W5S (highly sensitive to nitrogen oxides), W3C (sensitive to aromatic compounds, ammonia), W6S (sensitive to hydrogen), W5C (sensitive to olefin, short-chain aromatic compounds), W1S (sensitive to methyl), W1W (sensitive to sulfur compounds), W2S (sensitive to alcohols, aldehydes, and ketones), W2W (sensitive to organic sulfides), and W3S (sensitive to long-chain alkanes). RHX-MRPs mean rice protein isolate hydrolysate-xylose Maillard reaction products, and RHX-80, RHX-100, RHX-120, and RHX-140 represent RHX-MRPs prepared at different temperatures of 80, 100, 120, and 140 °C, respectively. RHXC-MRPs mean rice protein isolate hydrolysate-xylose-cysteine Maillard reaction products, and RHXC-80, RHXC-100, RHXC-120, and RHXC-140 represent RHXC-MRPs prepared at different temperatures of 80, 100, 120, and 140 °C, respectively. The clean air is used as the blank sample for E-nose analysis and umami solution consisting of 0.5% (*w/v*) sodium chloride (NaCl) and 1.0% (*w/v*) monosodium glutamate (MSG) is used as the blank sample for E-tongue analysis.

W5C, W3S, and W6S. RHX-MRPs displayed a positive correlation with the sensor signals of W1S, W2S, and W5S, while RHXC-MRPs were notably associated with the sensor signals of W1W and W2W. The phenomenon further proved that the absence of cysteine made for the formation of alcohols, aldehydes, ketones, and nitrogen oxides. Conversely, the addition of cysteine benefited the production of sulfur-containing compounds.

3.8. Analysis of taste attributes using E-tongue

The E-tongue can respond to basic taste attributes including sourness, astringency, bitterness, aftertaste-A (the duration of astringency in the mouth), aftertaste-B (the duration of bitterness in the mouth), umami, richness, and saltiness. As shown in the radar diagram of E-tongue (Fig. 5b), there was a stronger intensity of bitterness, umami,

richness, and saltiness perceived in RPIH-MRPs. All RPIH-MRPs showed lower bitterness but higher umami, richness, and saltiness properties compared to the blank, suggesting the umami and saltiness enhancement of MRPs (Yu et al., 2018). The intensity of bitterness and umami increased initially and then decreased as the temperature rose from 80 °C to 140 °C. The bitterness and umami in RHXC-MRPs were weaker than those in RHX-MRPs, which seemed to be inconsistent with the changes in bitter FAA and umami FAA. It might can be explained that the short peptides formed in MRPs had a positive influence on the improvement of umami, bitterness, and mouthfulness, which exhibited a greater effect than free amino acids (Ni et al., 2022). The reduction of bitterness/umami with the increase in temperature might be ascribed to the thermal degradation of some bitter/umami amino acids and bitter/umami peptides, and adding cysteine could help restrain the peptide cross-linking process, preventing the formation of bitter/umami peptides (He et al., 2019; Karangwa et al., 2015). Moreover, the richness and saltiness of RHXC-MRPs increased with rising temperature were stronger than those of RHX-MRPs, and RHXC-120 exhibited the strongest richness and saltiness.

For an improved visualization of the E-tongue data, PCA was performed to identify the discrimination of RPIH-MRPs based on variables related to various temperatures and cysteine levels. As shown in the score plot (Fig. 5e), PC1 and PC2 explained 80% of the overall variance, and the blank, RHX-MRPs, and RHXC-MRPs could be distinguished from each other. However, the differentiation of products prepared at different temperatures was not obvious, indicating that cysteine might have a more significant effect on the taste attributes of RPIH-MRPs. The result was further confirmed in the loading plot (Fig. 5f), where RHX-MRPs appeared to have a relatively stronger bitter and umami taste compared to RHXC-MRPs based on their location distribution.

3.9. Descriptive sensory analysis of RPIH-MRPs

As presented in Table 2, the mouthfulness and continuity significantly ($p < 0.05$) increased as the temperature rose from 80 °C to 120 °C, but then began to decline when the temperature reached 140 °C. RHXC-MRPs had better mouthfulness and continuity than RHX-MRPs, confirming the taste enhancement of cysteine (Zhao et al., 2019). The changes in umami and bitterness were consistent with the results of the E-tongue analysis, and RHX-100 had the highest umami and bitterness, followed by RHXC-100. As reported, the relatively low temperature (around 110 °C) facilitated the formation of umami, mouthfulness, and continuity (Wei et al., 2019). Moreover, the Maillard reaction can convert small peptides into cross-linking products of glycated peptides called "Maillard peptide", which can enhance umami, mouthfulness, and continuity (Yu et al., 2018). The weaker bitterness of the MRPs might be attributed to the masking effect of Maillard peptides

(Karangwa et al., 2015). Additionally, the saltiness among different RPIH-MRPs showed a non-significant ($p > 0.05$) difference, and the sensory scores ranged between 7.54 and 7.96 points.

Most notably, there was no significant ($p > 0.05$) difference in the meaty scores among RHX-MRPs. The meaty scores of RHXC-MRPs were significantly ($p < 0.05$) higher than those of RHX-MRPs, suggesting that adding cysteine was conducive to improving the meaty aroma. As the temperature increased, the meaty aroma of RHXC-MRPs initially rose and then declined, with RHXC-120 scoring the highest at 8.03 points. The meat-like flavor might be attributed to the higher concentration of sulfur-containing compounds such as 2-methyl-thiophene, 2,5-dimethyl-thiophene, 2-thiophenecarboxaldehyde, 2,5-thiophenedicarboxaldehyde, 3-methyl-2-thiophenecarboxaldehyde, thieno[3,2-*b*]thiophene, 2-methyl-thiazole, 2-furfurylthiol, 2-methyl-3-furanthiol, furfuryl sulfide, and bis(2-furfuryl)disulfide (Du et al., 2023; Xu et al., 2011). The caramel-like flavor increased initially and then decreased with a rise in temperature, and RHX-MRPs had a stronger caramel-like flavor compared to RHXC-MRPs, probably due to the formation of a higher content of furans and pyrazines (Karangwa et al., 2015). As an undesirable odor, the burnt odor increased significantly ($p < 0.05$) with increasing temperature, especially when the temperature reached 140 °C. After adding cysteine, the burnt odor of RHXC-MRPs was weakened compared to RHX-MRPs. Overall, RHXC-120 had the highest overall acceptance due to its relatively high mouthfulness, continuity, umami, meaty aroma, and relatively low bitterness.

3.10. Correlation analysis among free amino acids, volatile compounds, antioxidant activity, and sensory attributes

The correlation between volatile compounds and antioxidant activity was established for RHX-MRPs and RHXC-MRPs. As shown in the PCA loading plots (Fig. 6a and c), PC1 and PC2 together explained 77% of the overall variance. RHX-120 was clustered with reducing power and DPPH radical scavenging, positioned on the negative axis of PC1 (Fig. 6a). The same distribution of RHXC-120 was observed in Fig. 6c. The results further verified that RPIH-MRPs obtained at 120 °C exhibited stronger antioxidant activity, consistent with a study indicating that soybean peptide-MRPs prepared at 120 °C had ideal antioxidant properties (Yu et al., 2018). According to the clustering results, the DPPH radical scavenging ability and reducing power of RHX-120 were positively related to the furan, 2-ethyl-furan, 2,5-dimethyl-pyrazine, 2-(methoxymethyl)-furan, 2-furanmethanol, 2-pyrrolidinone, 2(1H)-pyridinone, 2-methyl-thiazole, and 2-thiophenecarboxaldehyde (Fig. 6b), while those of RHXC-120 were positively correlated with pyridine, 1-butyl-1H-pyrrole, 2-ethyl-furan, 2-methyl-furan, 2,6-dimethyl-pyrazine, 1-(2-furanyl)-ethanone, 2-acetylthiazole, 2-thiophenecarboxaldehyde, 2,5-thiophenedicarboxaldehyde, 2,3-dimethyl-thiophene,

Table 2

Effects of temperature and cysteine on the descriptive sensory attributes of RHX-MRPs and RHXC-MRPs.

Sensory attributes	Sensory score							
	RHX-80	RHX-100	RHX-120	RHX-140	RHXC-80	RHXC-100	RHXC-120	RHXC-140
Mouthfulness	4.13 ± 0.38[g]	6.05 ± 0.39[e]	7.58 ± 0.36[b]	6.28 ± 0.22[de]	4.54 ± 0.33[f]	6.46 ± 0.33[d]	7.95 ± 0.32[a]	7.22 ± 0.22[c]
Continuity	4.42 ± 0.36[f]	5.58 ± 0.36[d]	7.25 ± 0.26[a]	6.04 ± 0.33[c]	4.97 ± 0.31[e]	6.23 ± 0.21[c]	7.50 ± 0.37[a]	6.83 ± 0.21[b]
Umami	6.64 ± 0.37[cd]	7.58 ± 0.29[a]	7.21 ± 0.26[b]	6.54 ± 0.33[cd]	6.45 ± 0.31[de]	7.21 ± 0.20[b]	6.78 ± 0.22[c]	6.17 ± 0.18[e]
Bitterness	5.50 ± 0.43[b]	5.96 ± 0.33[a]	5.13 ± 0.23[c]	4.74 ± 0.23[d]	4.77 ± 0.21[d]	5.28 ± 0.22[bc]	4.58 ± 0.29[d]	4.24 ± 0.23[e]
Salty	7.54 ± 0.33[a]	7.67 ± 0.39[a]	7.66 ± 0.37[a]	7.58 ± 0.36[a]	7.88 ± 0.23[a]	7.92 ± 0.36[a]	7.96 ± 0.33[a]	7.83 ± 0.39[a]
Meaty	4.04 ± 0.33[f]	4.49 ± 0.34[e]	4.63 ± 0.43[e]	4.83 ± 0.21[e]	5.29 ± 0.33[d]	6.81 ± 0.21[c]	8.03 ± 0.33[a]	7.28 ± 0.22[b]
Caramel	6.04 ± 0.33[d]	6.83 ± 0.39[b]	7.85 ± 0.19[a]	6.96 ± 0.33[b]	4.88 ± 0.23[e]	6.21 ± 0.26[cd]	6.88 ± 0.38[b]	6.46 ± 0.33[c]
Burnt	4.54 ± 0.26[f]	6.54 ± 0.40[d]	7.50 ± 0.30[b]	8.43 ± 0.28[a]	4.03 ± 0.33[g]	5.08 ± 0.36[e]	6.58 ± 0.36[d]	7.13 ± 0.38[c]
Overall acceptance	5.42 ± 0.36[d]	6.42 ± 0.42[c]	7.29 ± 0.33[b]	6.08 ± 0.36[c]	4.96 ± 0.36[e]	5.08 ± 0.36[e]	8.24 ± 0.23[a]	7.03 ± 0.32[b]

Results are expressed as mean ± standard deviation (n = 3), values followed by different superscript lowercase letters in the same column mean statistically significant ($p < 0.05$) differences. RHX-MRPs mean rice protein isolate hydrolysate-xylose Maillard reaction products, and RHX-80, RHX-100, RHX-120, and RHX-140 represent RHX-MRPs prepared at different temperatures of 80, 100, 120, and 140 °C, respectively. RHXC-MRPs mean rice protein isolate hydrolysate-xylose-cysteine Maillard reaction products, RHXC-80, RHXC-100, RHXC-120, and RHXC-140 represent RHXC-MRPs prepared at different temperatures of 80, 100, 120, and 140 °C, respectively.
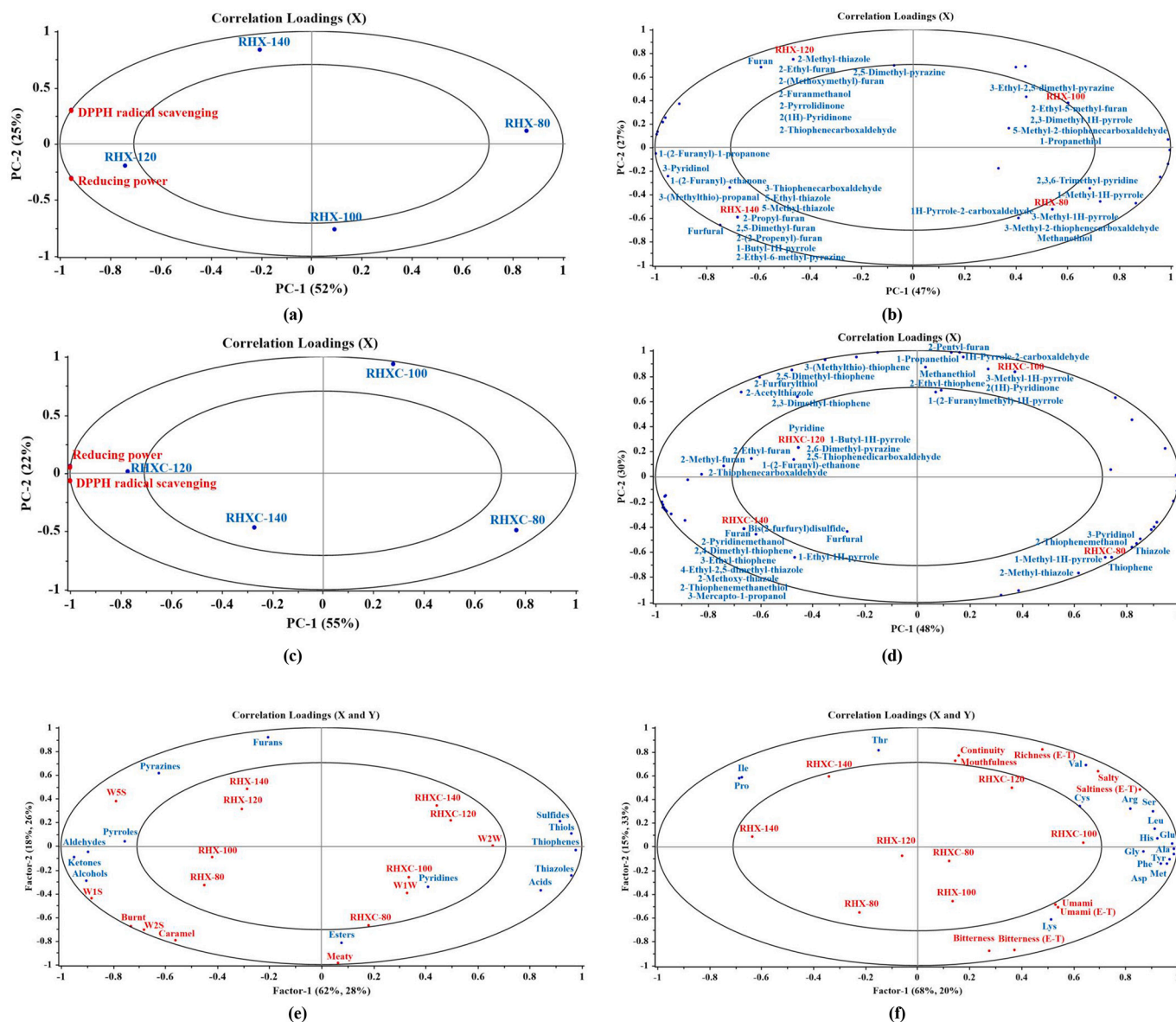
Fig. 6. The correlation analysis among free amino acids, volatile compounds, antioxidant activity, instrumental sensory data (E-nose and E-tongue), and descriptive sensory evaluation through PCA and PLSR analysis: (a) and (b) PCA correlation loading plot between volatile compounds and antioxidant activity for RHX-MRPs, (c) and (d) PCA correlation loading plot between volatile compounds and antioxidant activity for RHXC-MRPs, (e) PLSA correlation loading plot between volatile compounds, E-nose, and descriptive sensory evaluation, and (f) PLSA correlation loading plot between free amino acids, E-tongue, and descriptive sensory evaluation. For Fig. 6(e), the X-matrix is designed using GC–MS data, while the Y-matrix is designed using E–nose (W5S, W1S, W2S, W1W, and W2W) and descriptive sensory attributes (burnt, caramel, and meaty), respectively. For Fig. 6(f), the X-matrix is designed using FAA content, while the Y-matrix is designed using E–tongue (bitterness, umami, saltiness, and richness) and descriptive sensory attributes (mouthfulness, continuity, umami, bitterness, and salty), respectively. E-T means taste sensors of E–tongue.

2,5-dimethyl-thiophene, 3-(methylthio)-thiophene, and 2-furfurylthiol (Fig. 6d), which can be confirmed by previous studies (Huang et al., 2011; Yu et al., 2013). Compared with RHX-MRPs, the more prominent antioxidant activity of RHXC-MRPs seemed to stem from specific thiazoles, thiophenes, and thiols that were produced by adding cysteine.

On the other hand, the correlation among FAA, volatile compounds, instrumental sensory data (E-nose and E-tongue), and descriptive sensory evaluation was studied using the PLSR. PLSR has been effectively used to explain the correlation between variables by extracting information from raw data and focusing on a comprehensive evaluation of these information (Chen et al., 2018). For the PLSA loading plot (Fig. 6e), the X-matrix was designed using GC–MS data, while the Y-matrix was designed using E–nose (W5S, W1S, W2S, W1W, and W2W) and descriptive sensory attributes (burnt, caramel, and meaty),

respectively. The explained variance for X variables was 62% for Factor 1 and 18% for Factor 2, while for Y variables, the explained variance of the model was 28% for Factor 1 and 26% for Factor 2. It can be observed that RHXC-80, RHXC-100, RHXC-120, RHXC-140, meaty, W1W, W2W, sulfides, thiols, thiophenes, thiazoles, pyridines, acids, and esters were clustered and located on the right side of the plot, indicating that RHXC-MRPs showed more meaty flavor due to the presence of sulfides, thiols, thiophenes, and thiazoles. The result can be confirmed by the E-nose, as the W1W and W2W sensors showed a stronger response to RHXC-MRPs. In addition, RHX-80, RHX-100, RHX-120, RHX-140, burnt, caramel, furans, pyrroles, aldehydes, ketones, alcohols, pyrazines, W1S, W2S, and W5S were clustered and distributed on the left side of the plot, suggesting that RHX-MRPs had more aldehydes, ketones, alcohols, furans, pyrroles, and pyrazines, which contributed to the burnt and caramel

odor. The E-nose results further validated the production of aliphatic oxygen-containing compounds and nitrogen oxides.

As shown in Fig. 6f, the X-matrix was designed to represent FAA content, while the Y-matrix was designed to represent E–tongue (bitterness, umami, saltiness, and richness) and descriptive sensory attributes (mouthfulness, continuity, umami, bitterness, and salty), respectively. The sensors of the E-tongue were in good agreement with the attributes of descriptive sensory evaluation due to their relatively close spatial distribution. RHXC-120 had a close relation with mouthfulness and continuity, which were also considered as richness. Moreover, the content of umami FAA (Glu and Asp) and bitter FAA (Arg, Leu, His, Tyr, Phe, and Met) made a significant contribution to RHXC-100, which confirmed the variations in FAA and indicated that RHXC-100 had relatively high umami but also exhibited a stronger bitterness.

4. Conclusion

In summary, temperature and cysteine were confirmed as the significant processing variables affecting the formation of meaty flavor during the Maillard reaction. For the preparation of rice protein isolate hydrolysate MRPs, high temperatures could intensify the color, enhance the formation of volatile compounds and undesirable burnt odor, and diminish the overall umami and bitterness. Cysteine, as an essential flavor precursor, played a significant role in inhibiting color, enhancing antioxidant activity, and forming sulfur compounds such as sulfur-containing furans, thiophenes, thiazoles, thiols, and sulfides that contributed to the meaty flavor. Moreover, adding cysteine could enhance the mouthfulness, continuity, richness, and saltiness, but decrease bitterness. Overall, rice protein isolate hydrolysate MRPs prepared at 120 °C in the presence of cysteine exhibited the highest antioxidant activity and optimal taste and meaty flavor, making it a promising option for meaty flavor enhancement. The results would be valuable in the natural flavor industry, utilizing rice protein isolate as an alternative plant source for the production of meat flavoring.

CRediT authorship contribution statement

Zuoyong Zhang: Writing – original draft, Methodology, Investigation, Funding acquisition, Conceptualization. **Jiayi Chen:** Validation, Resources. **Li Zheng:** Validation, Resources. **Jinlong Zhao:** Validation, Resources. **Na Guo:** Validation, Resources, Funding acquisition. **Xue Fang:** Validation, Resources. **Xuan Lu:** Validation, Resources. **Fangyan Zhang:** Validation, Resources. **Guilan Zhu:** Writing – review & editing, Supervision, Project administration, Funding acquisition.

Declaration of competing interest

The authors declare that they have no known competing financial interests or personal relationships that could have appeared to influence the work reported in this paper.

Data availability

Data will be made available on request.

Acknowledgments

References

Cao, C., Sun, H., Song, X., Zhao, M., Lin, W., Sun, W., … Su, G. (2023). Effect of fermentation with *Tetragenococcus halophilus* and *Zygosaccharomyces rouxii* on selected non-volatile taste compounds in soybean protein hydrolysates. *LWT-Food. Science and Technology, 184*, Article 115053.

Cao, C., Xie, J., Hou, L., Zhao, J., Chen, F., Xiao, Q., Zhao, M., & Fan, M. (2017). Effect of glycine on reaction of cysteine-xylose: Insights on initial Maillard stage intermediates to develop meat flavor. *Food Research International, 99*, 444–453.

Chen, X., Yu, J., Cui, H., Xia, S., Zhang, X., & Yang, B. (2018). Effect of temperature on flavor compounds and sensory characteristics of Maillard reaction products derived from mushroom hydrolysate. *Molecules, 23*(2), Article 247.

Cheng, Y.-H., Mu, D.-C., Jiao, Y., Xu, Z., & Chen, M.-L. (2021). Microwave-assisted maillard reaction between rice protein and dextran induces structural changes and functional improvements. *Journal of Cereal Science, 97*, Article 103134.

Chiang, J. H., Yeo, M. T. Y., Ong, D. S. M., & Henry, C. J. (2022). Comparison of the molecular properties and volatile compounds of Maillard reaction products derived from animal-and cereal-based protein hydrolysates. *Food Chemistry, 383*, Article 132609.

Du, W., Wang, Y., Yan, Q., Bai, S., Huang, Y., Li, L., … Wang, F. (2023). The number and position of unsaturated bonds in aliphatic aldehydes affect the cysteine-glucose Maillard reaction: Formation mechanism and comparison of volatile compounds. *Food Research International, 173*, Article 113337.

Fu, Y., Liu, J., Zhang, W., Wæhrens, S. S., Tøstesen, M., Hansen, E. T., … Lametsch, R. (2020). Exopeptidase treatment combined with Maillard reaction modification of protein hydrolysates derived from porcine muscle and plasma: Structure–taste relationship. *Food Chemistry, 306*, Article 125613.

He, S., Zhang, Z., Sun, H., Zhu, Y., Zhao, J., Tang, M., Wu, X., & Cao, Y. (2019). Contributions of temperature and l-cysteine on the physicochemical properties and sensory characteristics of rapeseed flavor enhancer obtained from the rapeseed peptide and d-xylose Maillard reaction system. *Industrial Crops and Products, 128*, 455–463.

Huang, C., Cui, H., Hayat, K., Zhang, X., & Ho, C.-T. (2022). Variation of moisture state and taste characteristics during vacuum drying of Maillard reaction intermediates of hydrolyzed soybean protein and characterization of browning precursors via fluorescence spectroscopy. *Food Research International, 162*, Article 112086.

Huang, M., Liu, P., Song, S., Zhang, X., Hayat, K., Xia, S., Jia, C., & Gu, F. (2011). Contribution of sulfur-containing compounds to the colour-inhibiting effect and improved antioxidant activity of Maillard reaction products of soybean protein hydrolysates. *Journal of the Science of Food and Agriculture, 91*(4), 710–720.

Jin, W.-G., Du, Y.-N., Pei, J.-J., Zhao, J., Tang, Y., Shang, W.-H., Wu, H.-T., & Zhu, B.-W. (2018). Characterization and antioxidant activity of Maillard reaction products from a scallop (*Patinopecten yessoensis*) gonad hydrolysates-sugar model system. *Journal of Food Measurement and Characterization, 12*, 2883–2891.

Karangwa, E., Zhang, X., Murekatete, N., Masamba, K., Raymond, L. V., Shabbar, A., … Song, S. (2015). Effect of substrate type on sensory characteristics and antioxidant capacity of sunflower Maillard reaction products. *European Food Research and Technology, 240*, 939–960.

Lee, S. M., Kwon, G. Y., Kim, K.-O., & Kim, Y.-S. (2011). Metabolomic approach for determination of key volatile compounds related to beef flavor in glutathione-Maillard reaction products. *Analytica Chimica Acta, 703*(2), 204–211.

Ni, Z.-J., Liu, X., Xia, B., Hu, L.-T., Thakur, K., & Wei, Z.-J. (2021). Effects of sugars on the flavor and antioxidant properties of the Maillard reaction products of camellia seed meals. *Food Chemistry: X, 11*, Article 100127.

Ni, Z.-J., Wei, C.-K., Zheng, A.-R., Thakur, K., Zhang, J.-G., & Wei, Z.-J. (2022). Analysis of key precursor peptides and flavor components of flaxseed derived Maillard reaction products based on iBAQ mass spectrometry and molecular sensory science. *Food Chemistry: X, 13*, Article 100224.

Nooshkam, M., Varidi, M., & Bashash, M. (2019). The Maillard reaction products as food-born antioxidant and antibrowning agents in model and real food systems. *Food Chemistry, 275*, 644–660.

Shakoor, A., Zhang, C., Xie, J., & Yang, X. (2022). Maillard reaction chemistry in formation of critical intermediates and flavour compounds and their antioxidant properties. *Food Chemistry, 393*, Article 133416.

Shen, Y., Hu, L.-T., Xia, B., Ni, Z.-J., Elam, E., Thakur, K., … Wei, Z.-J. (2021). Effects of different sulfur-containing substances on the structural and flavor properties of defatted sesame seed meal derived Maillard reaction products. *Food Chemistry, 365*, Article 130463.

Sun, A., Chen, L., Wu, W., Soladoye, O. P., Zhang, Y., & Fu, Y. (2023). The potential meat flavoring generated from Maillard reaction products of wheat gluten protein hydrolysates-xylose: Impacts of different thermal treatment temperatures on flavor. *Food Research International, 165*, Article 112512.

Sun, A., Wu, W., Soladoye, O. P., Aluko, R. E., Bak, K. H., Fu, Y., & Zhang, Y. (2022). Maillard reaction of food-derived peptides as a potential route to generate meat flavor compounds: A review. *Food Research International, 151*, Article 110823.

Wang, X.-Y., Ma, Y.-J., Guo, Y., Luo, X.-L., Du, M., Dong, L., Yu, P., & Xu, X.-B. (2021). Reinvestigation of 2-acetylthiazole formation pathways in the Maillard reaction. *Food Chemistry, 345*, 128761.

Wei, C.-K., Ni, Z.-J., Thakur, K., Liao, A.-M., Huang, J.-H., & Wei, Z.-J. (2019). Color and flavor of flaxseed protein hydrolysates Maillard reaction products: Effect of cysteine, initial pH, and thermal treatment. *International Journal of Food Properties, 22*(1), 84–99.

Wei, C.-K., Thakur, K., Liu, D.-H., Zhang, J.-G., & Wei, Z.-J. (2018). Enzymatic hydrolysis of flaxseed (*Linum usitatissimum* L.) protein and sensory characterization of Maillard reaction products. *Food Chemistry, 263*, 186–193.

Xiao, Q., Woo, M. W., Hu, J., Xiong, H., & Zhao, Q. (2021). The role of heating time on the characteristics, functional properties and antioxidant activity of enzyme-hydrolyzed rice proteins-glucose Maillard reaction products. *Food Bioscience, 43*, Article 101225.

Xu, H., Zhang, X., Karangwa, E., & Xia, S. (2017). Correlating enzymatic browning inhibition and antioxidant ability of Maillard reaction products derived from different amino acids. *Journal of the Science of Food and Agriculture, 97*(12), 4210–4218.

Xu, Y., Chen, Q., Lei, S., Wu, P., Fan, G., Xu, X., & Pan, S. (2011). Effects of lard on the formation of volatiles from the Maillard reaction of cysteine with xylose. *Journal of the Science of Food and Agriculture, 91*(12), 2241–2246.

Yu, A.-N., Tan, Z.-W., & Wang, F.-S. (2012). Mechanism of formation of Sulphur aroma compounds from L-ascorbic acid and L-cysteine during the Maillard reaction. *Food Chemistry, 132*(3), 1316–1323.

Yu, H., Seow, Y.-X., Ong, P. K., & Zhou, W. (2017). Effects of high-intensity ultrasound on Maillard reaction in a model system of d-xylose and l-lysine. *Ultrasonics Sonochemistry, 34*, 154–163.

Yu, M., He, S., Tang, M., Zhang, Z., Zhu, Y., & Sun, H. (2018). Antioxidant activity and sensory characteristics of Maillard reaction products derived from different peptide fractions of soybean meal hydrolysate. *Food Chemistry, 243*, 249–257.

Yu, X., Zhao, M., Hu, J., Zeng, S., & Bai, X. (2012). Correspondence analysis of antioxidant activity and UV–vis absorbance of Maillard reaction products as related to reactants. *LWT-Food Science and Technology, 46*(1), 1–9.

Yu, X., Zhao, M., Liu, F., Zeng, S., & Hu, J. (2013). Antioxidants in volatile Maillard reaction products: Identification and interaction. *LWT-Food Science and Technology, 53*(1), 22–28.

Zhang, D., Ji, W., Peng, Y., Ji, H., & Gao, J. (2020). Evaluation of flavor improvement in Antarctic krill defluoridated hydrolysate by Maillard reaction using sensory analysis, E-nose, and GC-MS. *Journal of Aquatic Food Product Technology, 29*(3), 279–292.

Zhang, W., Han, Y., Shi, K., Wang, J., Yang, C., & Xu, X. (2022). Effect of different sulfur-containing compounds on the structure, sensory properties and antioxidant activities of Maillard reaction products obtained from *Pleurotus citrinopileatus* hydrolysates. *LWT-Food. Science and Technology, 171*, 114144.

Zhang, Z., He, S., Zhang, L., Li, X., Jin, R., Liu, Q., Chen, S., Wang, J., & Sun, H. (2022). The potential application of vegetable oils in the D-xylose and L-cysteine Maillard reaction system for meaty aroma production. *Food Research International, 155*, 111081.

Zhang, Z., Jiang, J., Zang, M., Zhang, K., Li, D., & Li, X. (2022). Flavor profile analysis of instant and traditional Lanzhou beef bouillons using HS-SPME-GC/MS, electronic nose and electronic tongue. *Bioengineering, 9*(10), 582.

Zhang, Z., Zang, M., Zhang, K., Wang, S., Li, D., & Li, X. (2021). Effects of phospholipids and reheating treatment on volatile compounds in phospholipid-xylose-cysteine reaction systems. *Food Chemistry, 139*, Article 109918.

Zhao, J., Wang, T., Xie, J., Xiao, Q., Du, W., Wang, Y., Cheng, J., & Wang, S. (2019). Meat flavor generation from different composition patterns of initial Maillard stage intermediates formed in heated cysteine-xylose-glycine reaction systems. *Food Chemistry, 274*, 79–88.

Zheng, A.-R., Wei, C.-K., Liu, D.-H., Thakur, K., Zhang, J.-G., & Wei, Z.-J. (2023). GC-MS and GC×GC-ToF-MS analysis of roasted/broth flavors produced by Maillard reaction system of cysteine-xylose-glutamate. *Current Research in Food. Science, 6*, Article 100445.

Zheng, Z., Zhang, L., Zhang, M., Mujumdar, A. S., & Liu, Y. (2023). Maillard reaction products of pea protein hydrolysate as a flavour enhancer for beef flavors: Effects on flavor and physicochemical properties. *Food Chemistry, 417*, Article 135769.

Zhu, J., Xia, X., Zhang, F., Song, S., Cui, H., Hayat, K., … Ho, C.-T. (2023). Taste characteristic and the mechanism of light-colored Maillard reaction products derived from gluten hydrolysate. *Food Bioscience, 52*, Article 102394.